Double scattering in critically opalescent fluids

J. G. Shanks* and J. V. Sengers
Institute for Physical Science and Technology and Department of Physics and Astronomy, University of Maryland, College Park, Maryland 20742
(Received 7 January 1988)

A procedure is presented for the calculation of the intensity of light doubly scattered by a critically opalescent fluid. The procedure is valid for general scattering angles and fully incorporates the effect of turbidity on the double-scattered light. The intensity and depolarization ratio of double-scattered light is evaluated as a function of temperature, angle, and sample-cell dimensions for some representative liquid mixtures near the critical point of mixing. A comparison with experimental multiple-scattering data is also included.

I. INTRODUCTION

Light scattering provides an important tool for studying critical fluctuations in fluids.[1,2] The intensity of (singly) scattered light is directly proportional to the Fourier transform of the order-parameter correlation function. The primary limitation of the interpretation of such light-scattering experiments is the appearance of double and higher-order scattering close to the critical point.[3] As a consequence, light-scattering data collected by modern multiangle photometers[4,5] require an angle-dependent correction for double scattering in critically opalescent fluids.

Attempts have been made to minimize multiple scattering. One approach, adopted in our laboratory,[6–8] is to select a mixture of liquids, such as 3-methylpentane and nitroethane, whose refractive indices differ only slightly, so that the coupling between dielectric-constant and order-parameter fluctuations is weak. Another approach is to perform light-scattering experiments with a very small sample volume as was done by Kopelman *et al.*[9] However, even in these special cases, corrections due to double scattering must be applied within the experimentally accessible temperature range near the critical point.

Double-scattering effects in fluids near the critical point have been considered by a number of investigators. Oxtoby and Gelbart[10,11] estimated the effect of double scattering on the polarized and depolarized light-scattering intensity from an order-parameter correlation function which was assumed to be independent of the wave number k, and neglecting any attenuation of the light beam due to the turbidity of the sample. They pointed out that the collision-induced contribution to the depolarization ratio of a fluid may be small compared to that of double scattering, and concluded that the depolarization ratio varies linearly with the height of the volume observed by the detector.[10] For this purpose Oxtoby and Gelbart considered a spherical scattering volume in a spherical cell. This geometry is physically unrealizable and Reith and Swinney[12] extended the analysis to the more realistic cylindrical scattering geometry. A more detailed analysis of the double-scattering effects in a cylindrical sample cell was made by Bray and Chang[13] taking into account the k dependence of the order-parameter correlation function. Like Reith and Swinney, Bray and Chang restricted their analysis to 90° scattering and neglected turbidity losses. Boots, *et al.*[14] and Boots[15] developed a systematic theory of multiple scattering valid for all scattering angles; in practice they restricted themselves to the regime where turbidity and double-scattering effects are small. The theory was used to make a comparison with experimental depolarization ratios at 90° observed by Trappeniers and co-workers[16–18] for xenon and carbon dioxide near the vapor-liquid critical point. Experimental studies of multiple-scattering effects in binary-liquid mixtures near the consolute point have been reported by Hamano *et al.*[19] and by Schroeter *et al.*[20] The work of Schroeter *et al.* includes an assessment of diffraction effects attendant to the use of small apertures. Studies of double-scattering effects have also been reported by several Russian investigators.[21–23]

Because of the complexity of the problem, a number of restrictions or approximations are commonly introduced in the analysis of double-scattering effects. Some of the investigators have restricted the analysis to 90° scattering.[12,13,16–18,20] The effect of turbidity on the double scattering has either been neglected completely[10–13,20] or approximations have been made so that the analysis is restricted to conditions where turbidity losses in the cell are small.[14,15,21,22]

In this paper we consider light scattered from a fluid in a cylindrical cell. We shall present an improved analysis valid for all scattering angles and fully incorporating the effect of the turbidity on the double-scattering intensity. In a fluid near the vapor-liquid critical point an added complication arises due to the presence of density gradients induced by gravity.[24] In practice, therefore, we apply our analysis to binary liquids near the critical mixing point, where the relaxation time for stratification is long and measurements from homogeneous fluid samples can be obtained.[6] Throughout this paper we shall consider

binary liquids whose composition is equal to the critical composition.

In this paper we restrict ourselves to an analysis of the double-scattering contributions to the polarized and depolarized light-scattering intensities. The dynamical features of the double-scattering spectrum of fluids near the critical point have been discussed by Sorensen *et al.*,[25,26] Beysens and Zalczer,[27] Ferrell and Bhattacharjee,[28] and Romanov and Salikhov.[29]

II. BASIC EQUATIONS FOR SINGLE AND DOUBLE SCATTERING

The differential cross section for light scattering or Rayleigh ratio is given by[30,31]

$$\sigma(\theta,\Phi)=\frac{\pi^2}{\lambda^4}V\sin^2\Phi\langle\,|\,\Delta\epsilon(k)\,|^2\rangle_V\ , \tag{2.1}$$

where λ is the vacuum wavelength of the light, V the scattering volume, Φ the angle between the polarization vector of the incident beam and the wave vector $\mathbf{k}_s$ of the scattered light, and $\langle\,|\,\Delta\epsilon(k)\,|^2\rangle_V$ the Fourier component of the dielectric-constant fluctuations in the volume V. The wave number k is related to that of the incident light k_0 and the scattering angle θ by

$$k=2k_0\sin(\theta/2)=(4\pi n/\lambda)\sin(\theta/2)\ , \tag{2.2}$$

where n is the refractive index of the medium. Near the critical point the dielectric-constant fluctuations are primarily caused by fluctuations in the order parameter associated with the phase transition which, for a liquid mixture near the consolute point, is the concentration X. For a system at the critical concentration and at temperatures T close to the critical temperature T_c, the concentration fluctuations satisfy a scaled equation of the form[1,2,32]

$$\langle\,|\,\Delta X(k)\,|^2\rangle_V=N^{-1}\Gamma t^{-\gamma}g(k\xi)\ , \tag{2.3}$$

where $N=\rho_c V$ is the number of molecules in volume V, Γ is a system-dependent constant, $t=(T-T_c)/T$, $\xi=\xi_0 t^{-\nu}$, the correlation length, while γ and ν are universal critical exponents, and $g(k\xi)$ a universal scaling function. For the purpose of this paper the scaling function $g(k\xi)$ is approximated by the Ornstein-Zernike form $g(k\xi)=(1+k^2\xi^2)^{-1}$, since any deviations from this form are very small.[6]

For our analysis we write the Rayleigh ratio in the form

$$\sigma(\theta,\Phi)=\frac{A\sin^2\Phi}{\alpha-\cos\theta}\ , \tag{2.4}$$

where

$$A=\frac{\pi^2}{\lambda^4}\left[\frac{\partial\epsilon}{\partial X}\right]_{T,P}^2\rho_c^{-1}\frac{\Gamma t^{-\gamma}}{2(k_0\xi)^2}\ , \tag{2.5}$$

and

$$\alpha=1+\frac{1}{2(k_0\xi)^2}\ . \tag{2.6}$$

Since $t^{-\gamma}/\xi^2$ varies with temperature as $t^{0.02}$, the coefficient A can in practice be treated as a constant independent of temperature. The total cross section or turbidity τ is obtained[13,33] by integrating (2.4) over all solid angles Ω,

$$\tau=\int d\Omega\,\sigma(\theta,\Phi)$$
$$=A\pi\left[(1+\alpha^2)\ln\left[\frac{\alpha+1}{\alpha-1}\right]-2\alpha\right]\ . \tag{2.7}$$

We consider an experimental arrangement in which the fluid is contained in a cylindrical sample cell with radius R and with its cylindrical axis in the positive Z direction. The incident beam is directed along the (negative) X axis and polarized in the Z direction, while the detector for the scattered light is located in the (X,Y) plane at a scattering angle θ. The detector images the light emanating from an acceptance volume V_a with width Δa ($\Delta a \ll R$) and height H. A top view of the arrangement is schematically shown in Fig. 1. We neglect the finite diameter of the incident beam relative to the height of the acceptance volume so that the incident intensity can be approximated by $I_0=P_0\delta(y)\delta(z)$, and we shall consider the scattered intensity relative to the incident power P_0. The intensity of singly scattered light observed by the detector is then proportional to

$$I^{(1)}(\theta,\Phi)=\sigma(\theta,\Phi)e^{-2\tau R}\Delta a/\sin\theta$$
$$=\frac{A\sin^2\Phi}{\alpha-\cos\theta}e^{-2\tau R}\frac{\Delta a}{\sin\theta}\ , \tag{2.8}$$

where we have accounted for the attenuation of the light beam over its path length $2R$ in the fluid.

The intensity of doubly scattered light observed by the detector is obtained by integrating over all paths in which the first scattering event with angles θ_1,Φ_1 is located at $\mathbf{r}_1=(x_1,0,0)$ on the X axis and the second scattering event with angles θ_2,Φ_2 at $\mathbf{r}_2=(x_2,y_2,z_2)$ in the acceptance volume V_a,

$$I^{(2)}(\theta)=\int_{V_a}d\mathbf{r}_2\int_{-R}^{+R}dx_1\frac{e^{-\tau l(\mathbf{r}_1,\mathbf{r}_2)}\sigma(\theta_1,\Phi_1)\sigma(\theta_2,\Phi_2)}{r_{21}^2}\ , \tag{2.9}$$

where $r_{21}=|\,\mathbf{r}_2-\mathbf{r}_1\,|$ is the distance between the scattering events and $l(\mathbf{r}_1,\mathbf{r}_2)$ the total path length of the light in

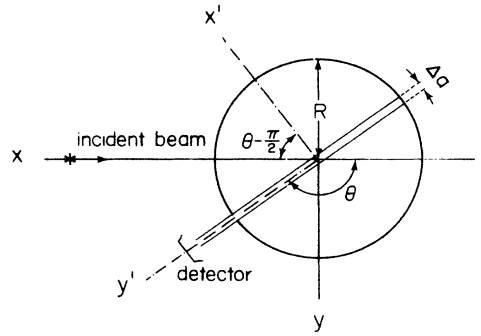

FIG. 1. Top view of scattering geometry.

the fluid. We find it convenient to rotate the axis in the (X,Y) plane over an angle $\theta-\pi/2$, so that the new Y' axis is located in the acceptance volume in the direction towards the detector. The volume element in (2.9) may then be replaced with $\Delta a\, dy_2'\, dz_2'\, dx_1'$, if we assume that the variation of the integrand over the width of the acceptance volume, i.e., for $-\Delta a/2 < x_2' < +\Delta a/2$, can be neglected. In the sequel we shall denote x_1 by u, y_2' by v, $z_2'=z_2$ by w, and r_{21} by ρ as indicated in Fig. 2, so that

$$r_{21}^2=\rho^2=u^2+v^2+w^2+2uv\cos\theta\ , \tag{2.10}$$

$$l(\mathbf{r}_1,\mathbf{r}_2)=2R+\rho-u-v\ . \tag{2.11}$$

Noting that $dx_1'=\sin\theta\, du$ and using (2.4), we write $I^{(2)}(\theta)$ as

$$I^{(2)}(\theta)=A^2\,\Delta a\sin\theta\, e^{-2R\tau}\times\int_{-R}^{+R}du\int_{-R}^{+R}dv\int_{-H/2}^{+H/2}dw\, G(u,v,w)\ , \tag{2.12}$$

with

$$G(u,v,w)=\frac{e^{\tau(u+v-\rho)}\sin^2\Phi_1\sin^2\Phi_2}{\rho^2(\alpha-\cos\theta_1)(\alpha-\cos\theta_2)}\ . \tag{2.13}$$

Let us designate the wave vectors $\hat{\mathbf{k}}_j$ and the polarization directions $\hat{\mathbf{p}}_j$ of the incident, singly scattered, and doubly scattered light by $(\mathbf{k}_0,\mathbf{p}_0)$, $(\mathbf{k}_1,\mathbf{p}_1)$, and $(\mathbf{k}_2,\mathbf{p}_2)$, respectively. We note that

$$\hat{\mathbf{k}}_0=-\hat{\mathbf{u}},\quad \hat{\mathbf{p}}_0=\hat{\mathbf{w}},\quad \hat{\mathbf{k}}_2=\hat{\mathbf{v}}\ ,$$

$$\hat{\mathbf{p}}_1=[\hat{\mathbf{p}}_0-(\hat{\mathbf{p}}_0\cdot\hat{\mathbf{k}}_1)\hat{\mathbf{k}}_1]/\sin\Phi_1\ ,$$

$$\hat{\mathbf{p}}_2=[\hat{\mathbf{p}}_1-(\hat{\mathbf{p}}_1\cdot\hat{\mathbf{k}}_2)\hat{\mathbf{k}}_2]/\sin\Phi_2\ .$$

For the trigonometric functions in (2.13) we obtain

$$\cos\theta_1=\hat{\mathbf{k}}_0\cdot\hat{\mathbf{k}}_1=\frac{u+v\cos\theta}{\rho}\ , \tag{2.14a}$$

$$\cos\theta_2=\hat{\mathbf{k}}_1\cdot\hat{\mathbf{k}}_2=\frac{u\cos\theta+v}{\rho}\ , \tag{2.14b}$$

$$\sin^2\Phi_1=1-(\hat{\mathbf{p}}_0\cdot\hat{\mathbf{k}}_1)^2=1-\frac{w^2}{\rho^2}\ , \tag{2.14c}$$

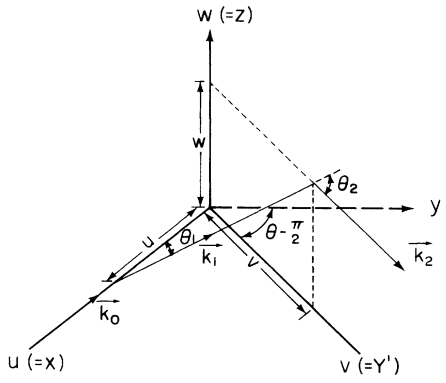

FIG. 2. A double-scattering trajectory.

$$\sin^2\Phi_2=1-(\hat{\mathbf{p}}_1\cdot\hat{\mathbf{k}}_2)^2=\frac{(\rho^2-w^2)^2+u^2w^2\sin^2\theta}{\rho^2(\rho^2-w^2)}\ . \tag{2.14d}$$

The integrand $G(u,v,w)$ of the double-scattering integral (2.12) can thus be written as

$$G(u,v,w)=\frac{e^{\tau(u+v-\rho)}(g_{vv}+g_{vh})}{(\alpha\rho-u-v\cos\theta)(\alpha\rho-u\cos\theta-v)}\ , \tag{2.15}$$

with

$$g_{vv}=\left[1-\frac{w^2}{\rho^2}\right]^2,\quad g_{vh}=\frac{u^2w^2}{\rho^4}\sin^2\theta\ . \tag{2.16}$$

The double-scattered intensity $I^{(2)}(\theta)$ is the sum of a polarized contribution $I_{vv}^{(2)}(\theta)$ for which $(\hat{\mathbf{p}}_0\cdot\hat{\mathbf{p}}_2)^2=\sin^2\Phi_1/\sin^2\Phi_2=1$ and a depolarized contribution $I_{vh}^{(2)}(\theta)$.

From the expressions (2.12), (2.15), and (2.16) we can draw the following conclusions. Since, as mentioned earlier, the temperature dependence of the coefficient A is negligibly small, the double-scattered intensity depends on the temperature through the turbidity τ, which increases rapidly as $T\to T_c$, and through α, which approaches unity as $T\to T_c$. If $\tau R>1$, the exponential term in (2.12) will significantly attenuate the scattering in all but the backscatter directions. In practical experiments $\rho\gg w$, so that $g_{vv}\gg g_{vh}$. Furthermore, g_{vv} is relatively insensitive to the scattering angle θ, so that the angular distribution of the polarized light is essentially fixed by the exponential factor and the denominator in (2.15). On the other hand, g_{vh} is proportional to ρ^{-4}, which increases strongly as $\theta\to\pi$; thus $I_{vh}^{(2)}$ will become large in the backscatter directions. Finally the w^2 factor in g_{vh} illustrates a general property of light multiply-scattered by isotropic-scattering centers: the depolarized component vanishes when the scattering process is restricted to the $w=0$ plane.

III. TRANSFORMATION OF DOUBLE-SCATTERING INTEGRAL

The double-scattering integral, as given by (2.12) and (2.15), cannot be evaluated analytically. To simplify the analysis, previous investigators have introduced a number of additional approximations. Bray and Chang[13] take $\tau=0$ and $\theta=\pi/2$, a simplification which enabled them to perform two of the integrations analytically, leaving the third to be evaluated numerically. Boots *et al.*,[14] Boots,[15] and Adzhemyan *et al.*[21,22] neglect the exponential factor in (2.15) and consider the double scattering under the assumption that $k_0\xi\ll 2R/H$. In this section we shall demonstrate how the double-scattering integral can be evaluated without any of these approximations.

As it stands, the three-dimensional double-scattering integral (2.12) is not well suited for numerical analysis because the integrand (2.15) has a singularity at $\rho=0$. However, it is possible to reduce the expression to a two-dimensional integral with a nonsingular integrand by changing coordinates. For this purpose we consider an orthogonal coordinate system $(u',v',w'=w)$ such that $\rho^2=u'^2+v'^2+w'^2$. In this new coordinate system we

then use polar coordinates with radius ρ, polar angle δ, and azimuthal angle ψ. This goal is accomplished by the following transformation:

$$u=\rho\frac{\sin\delta}{\sin\theta}\cos(\psi+\psi_0)\ , \tag{3.1a}$$

$$v=\rho\frac{\sin\delta}{\sin\theta}\sin(\psi-\psi_0)\ , \tag{3.1b}$$

$$w=\rho\cos\delta\ , \tag{3.1c}$$

with

$$\psi_0=\frac{\pi}{4}-\frac{\theta}{2}\ . \tag{3.2}$$

The Jacobian of this transformation is

$$\frac{\partial\{u,v,w\}}{\partial\{\rho,\delta,\psi\}}=\rho^2\frac{\sin\delta}{\sin\theta}\ , \tag{3.3}$$

and we obtain

$$I^{(2)}(\theta)=A^2\Delta a\, e^{-2R\tau}\int d\rho\int d\delta\int d\psi\, F(\rho,\delta,\psi)\ , \tag{3.4}$$

where

$$F(\rho,\delta,\psi)=\frac{[f_{vv}(\delta)+f_{vh}(\delta,\psi)]\sin\delta\exp\{\rho\tau[c_1(\psi)\sin\delta-1]\}}{[\alpha-c_2(\psi)\sin\delta][\alpha-c_3(\psi)\sin\delta]}\ , \tag{3.5}$$

with

$$f_{vv}(\delta)=\sin^4\delta\ ,$$
$$f_{vh}(\delta,\psi)=\tfrac{1}{4}\sin^2(2\delta)\cos^2(\psi+\psi_0)\ , \tag{3.6}$$

and

$$c_1(\psi)=[\cos(\psi+\psi_0)+\sin(\psi-\psi_0)]/\sin\theta\ , \tag{3.7a}$$

$$c_2(\psi)=[\cos(\psi+\psi_0)+\cos\theta\sin(\psi-\psi_0)]/\sin\theta\ , \tag{3.7b}$$

$$c_3(\psi)=[\sin(\psi-\psi_0)+\cos\theta\cos(\psi+\psi_0)]/\sin\theta\ . \tag{3.7c}$$

The singularity of the original integrand proportional to ρ^{-2} has been canceled by the factor ρ^2 in the Jacobian (3.3). The integration over ρ can now be done analytically and the remaining two-dimensional integral can be evaluated by standard numerical methods.

For computational efficiency it is advisable to take advantage of the symmetry of the integration limits in (2.12), so that this integral can be written as

$$I^{(2)}(\theta)=8A^2\Delta a\, e^{-2R\tau}\sin\theta \times\int_0^R du\int_0^R dv\int_0^{H/2} dw\,\tilde{G}(u,v,w)\ , \tag{3.8}$$

with

$$\tilde{G}(u,v,w)=\tfrac{1}{4}[G(u,v,w)+G(-u,v,w)+G(u,-v,w)+G(-u,-v,w)]\ . \tag{3.9}$$

In terms of the integration variables ρ,δ,ψ we obtain

$$I^{(2)}(\theta)=8A^2\Delta a\, e^{-2R\tau}\int_{[(\pi/2)-\theta]/2}^{[(\pi/2)+\theta]/2} d\psi\int_0^{\pi/2} d\delta\int_0^{\rho_{\max}(\delta,\psi)} d\rho\,\tilde{F}(\rho,\delta,\psi)\ , \tag{3.10}$$

with

$$\tilde{F}(\rho,\delta,\psi)=\rho^2\sin\delta\,\tilde{G}(u(\rho,\delta,\psi),v(\rho,\delta,\psi),w(\rho,\delta))\ . \tag{3.11}$$

The evaluation of $\tilde{F}(\rho,\delta,\psi)$ is tedious, but straightforward, and is documented elsewhere.[34] We obtain

$$\tilde{F}(\rho,\delta,\psi)=\sum_{i=1}^{4} e^{\rho\tau H_i(\delta,\psi)}[J_{vv}^{(i)}(\delta,\psi)+J_{vh}^{(i)}(\delta,\psi)]\ , \tag{3.12}$$

in terms of functions $H_i(\delta,\psi)$, $J_{vv}^{(i)}(\delta,\psi)$, and $J_{vh}^{(i)}(\delta,\psi)$, defined in the Appendix. Substitution of (3.12) into (3.10) yields the final form of the double-scattering integral

$$I^{(2)}(\theta)=8A^2\Delta a\, e^{-2R\tau}\sum_{i=1}^{4}\int_{[(\pi/2)-\theta]/2}^{[(\pi/2)+\theta]/2} d\psi\int_0^{\pi/2} d\delta\left[\frac{e^{\tau\rho_{\max}(\delta,\psi)H_i(\delta,\psi)}-1}{\tau H_i(\delta,\psi)}\right][J_{vv}^{(i)}(\delta,\psi)+J_{vh}^{(i)}(\delta,\psi)]\ . \tag{3.13}$$

The function $\rho_{\max}(\delta,\psi)$ is defined as follows. For a given ψ, i.e., a given ratio u/v, the maximum value $\rho'(\psi)$ of ρ,

$$\rho'(\psi)=\left[\frac{R^2\sin^2\theta}{\sin^2[\,|\psi-(\pi/4)|+\frac{1}{2}\theta]}+\left[\frac{H}{2}\right]^2\right]^{1/2} \tag{3.14}$$

occurs at

$$\delta'(\psi)=\arccos\left[\frac{H}{2\rho'(\psi)}\right]\ . \tag{3.15}$$

For general δ and ψ, $\rho_{\max}(\delta,\psi)$ is then given by

$$\rho_{\max}(\delta,\psi)=\begin{cases}\dfrac{R\sin\theta}{\sin\delta\sin[\,|\psi-(\pi/4)|+\frac{1}{2}\theta]} & \text{for } \delta'(\psi)<\delta<\pi/2\\ \dfrac{H}{2}\sec\delta & \text{for } 0<\delta<\delta'(\psi)\ .\end{cases} \tag{3.16}$$

The two-dimensional double-scattering integral (3.13) can be evaluated numerically with nested Gauss-Legendre quadrature algorithms. An accuracy of a few percent is achieved with a total of $(32)^2=1024$ integrand evaluations.

In practice we are interested in the ratio of the double-scattered intensity to the single-scattered intensity,

$$\hat{I}^{(2)}(\theta)\equiv I^{(2)}(\theta)/I^{(1)}(\theta)\ . \tag{3.17}$$

The depolarization ratio is defined as

$$\Delta^{(2)}(\theta)\equiv\frac{I_{vh}^{(2)}(\theta)}{I^{(1)}(\theta)+I_{vv}^{(2)}(\theta)}\ . \tag{3.18}$$

IV. ANALYSIS OF DOUBLE-SCATTERING EFFECTS

With tractable expressions in hand for the double-scattered intensity $\hat{I}^{(2)}$ and the depolarization ratio $\Delta^{(2)}$, we can readily investigate how these effects depend on experimental parameters such as the scattering angle θ, the temperature $t=(T-T_c)/T$, the size of the sample volume, i.e., the radius R, and the height H of the aperture. For this purpose we consider vertically polarized He-Ne laser light with an incident vacuum wavelength $\lambda=0.6328$ μm scattered through two representative liquid mixtures of different character, namely, 3-methylpentane + nitroethane and methanol + cyclohexane. The 3-methylpentane + nitroethane mixture is a weak scatterer, so that double-scattering effects will be small. With this system it is possible to perform accurate light-scattering experiments at temperatures very close to the critical temperature. The intensity of scattered light for this mixture has been measured in our laboratory[6,34] and also by Wiltzius and Cannell.[34,35] The methanol + cyclohexane system is a strong scatterer, so that double-scattering effects will be large. With this system it is not possible to obtain reliable information very close to the critical temperature unless one uses a sample cell with an ultrashort path length as was done by Kopelman *et al.*[9]

From (2.5) it follows that the coefficient A will vary with temperature as

$$A=\frac{A_0}{2(k_0\xi_0)^2}t^{2\nu-\gamma}\ , \tag{4.1}$$

where

$$A_0=\frac{\pi^2\Gamma}{\lambda^4\rho_c}\left[\frac{\partial\epsilon}{\partial x}\right]_{T,P}^2 \tag{4.2}$$

is the scattering strength. For the critical exponents γ and ν we adopt the values

$$\gamma=1.239,\quad \nu=0.63\ , \tag{4.3}$$

in good agreement with the current theoretical predictions.[36] In addition we need the critical temperature T_c, the correlation length ξ_0, the incident wave number k_0, which depends on the refractive index n, and the scattering strength A_0. The values adopted for these system-dependent quantities are presented in Table I. The physical parameters used for 3-methylpentane + nitroethane were deduced from the experimental data of Chang *et al.*,[6] and those for methanol + cyclohexane from the experimental data of Chu[37] and of Schroeter *et al.*[20] It should be noted that Kopelman *et al.*[9] and Jacobs[38] have measured the turbidity of methanol + cyclohexane, finding the slightly different values $\xi_0=0.39\pm0.1$ nm, $A_0=(3.0\pm0.3)\times10^{-4}$ m^{-1} and $\xi_0=0.324\pm0.006$ nm, $A_0=(2.20\pm0.04)\times10^{-4}$ m^{-1}, respectively. In Table I we have also included the corresponding quantities for diethylmalonate + polystyrene, to be discussed in Sec. V; the physical parameters for this system were obtained from the paper of Hamano *et al.*[19]

For a study of the double-scattering effects as a function of scattering angle and temperature we take $R=0.50$ cm and $H=0.062$ cm; these values correspond to the light-scattering photometer of Haller *et al.*[5] In Fig. 3 we show the double-scattered intensity $\hat{I}^{(2)}$ and the depolarization ratio $\Delta^{(2)}$ for 3-methylpentane + nitroethane as a function of the scattering angle θ at various values of the temperature difference $\Delta T=T-T_c$. From Fig. 3(a) we note that the double-scattered intensity $\hat{I}^{(2)}$ for this system at $\Delta T=10$ mK is less than 1% at all scattering angles. In Fig. 3(a) we have included a curve of $\hat{I}^{(2)}$ at $\Delta T=0.01$ mK; this was done to indicate that nothing surprising occurs even when $k_0\xi\simeq160$. From Fig. 3(b) we note that the depolarization ratio $\Delta^{(2)}$ is extremely small for a weak scatterer such as 3-methylpentane + nitroethane.

TABLE I. Physical parameters for some binary-liquid mixtures.

	3-methylpentane + nitroethane[a]	Methanol + cyclohexane[b]	Diethylmalonate + polystyrene[c]
T_c	299.545 K	318.62 K	283.82 K
ξ_0	0.229 nm	0.36 nm	1.00 nm
k_0	1.367×10^{7} m^{-1}	1.370×10^{7} m^{-1}	1.421×10^{7} m^{-1}
A_0	4.11×10^{-6} m^{-1}	3.7×10^{-4} m^{-1}	5.63×10^{-3} m^{-1}

[a]Reference 6.
[b]References 20 and 37.
[c]Reference 19.

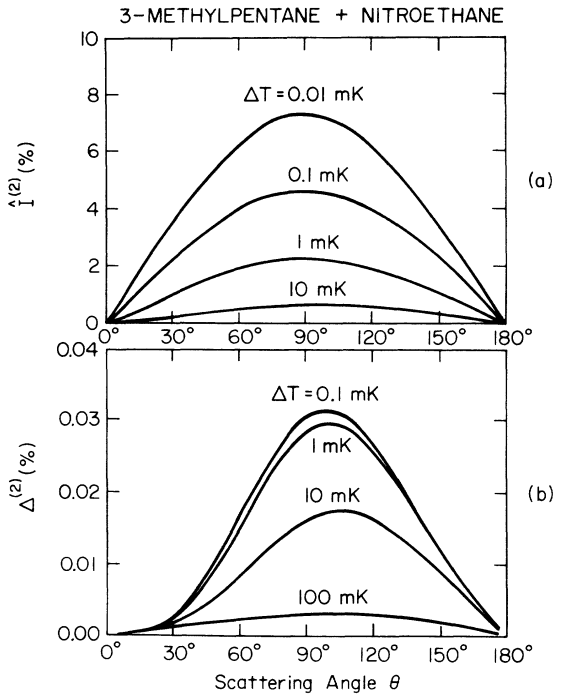

FIG. 3. Double-scattered intensity $\hat{I}^{(2)}$ and depolarization ratio $\Delta^{(2)}$ for 3-methylpentane + nitroethane as a function of the scattering angle θ at various values of $\Delta T = T - T_c$. ($R = 0.50$ cm, $H = 0.062$ cm.)

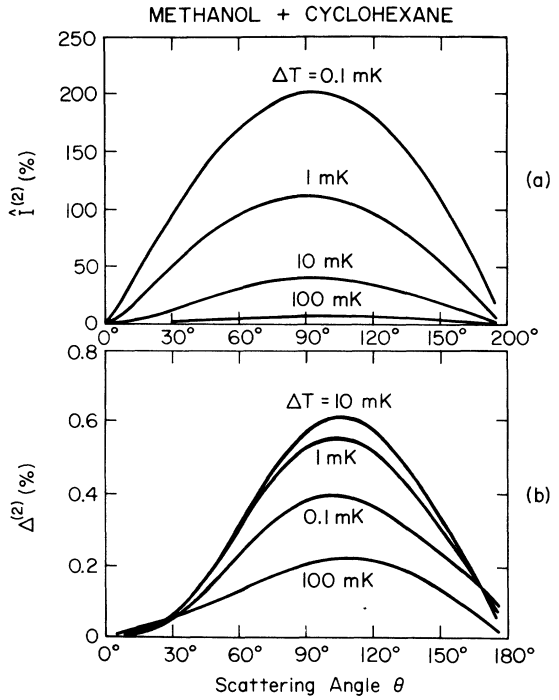

FIG. 4. Double-scattered intensity $\hat{I}^{(2)}$ and depolarization ratio $\Delta^{(2)}$ for methanol + cyclohexane as a function of the scattering angle θ at various values of $\Delta T = T - T_c$. ($R = 0.50$ cm, $H = 0.062$ cm.)

In Fig. 4 we present the corresponding information for methanol + cyclohexane. In a strong scatterer such as methanol + cyclohexane the double-scattering intensity $\hat{I}^{(2)}$ becomes very large and also the depolarization ratio $\Delta^{(2)}$ becomes appreciable. Of course, when the double-scattered intensity becomes comparable to the single-scattered intensity, we must expect significant additional contributions from higher-order scattering. From Figs. 3(a) and 4(a) we note that $\hat{I}^{(2)}$ appears to be roughly symmetric about 90° except at $\Delta T = 100$ mK. To explain this behavior it is convenient to consider three regimes. First, when $k_0\xi \ll 1$, both $I^{(1)}$ and $I^{(2)}$ will be essentially isotropic, so that $\hat{I}^{(2)}$ will be symmetric. When $k_0\xi$ is of order unity, $I^{(1)}$ at $\theta = 45°$ is about three times larger than $I^{(1)}$ at $\theta = 135°$, while $I^{(2)}$ is still relatively isotropic. As a consequence, $\hat{I}^{(2)}$ exhibits a distinct asymmetry, as is the case at $\Delta T = 100$ mK. Finally, when $k_0\xi \gg 1$, most of the single-scattered light is thrown into a narrow cone about $\theta = 0°$; most of the observed double-scattered light has been scattered into the detector from the intersection of this cone with the acceptance volume, a volume section nearly coincident with the center of the cell, i.e., the location of the single-scattering events. Thus $I^{(2)}$ will be roughly proportional to $I^{(1)}$, so that $\hat{I}^{(2)}$ becomes again symmetric.

The above considerations are no longer valid when the turbidity losses through the cell are large. In Fig. 5 we show $\hat{I}^{(2)}(\theta)$ of methanol + cyclohexane at $\Delta T = 10$ mK for different values of the sample radius R. As the radius R ranges from values smaller than τ^{-1} to values larger than τ^{-1}, the distribution of the double-scattered light changes in two distinct ways. $\hat{I}^{(2)}$ at $\theta = 90°$ increases roughly as the square root of the radius R, while the asymmetry about $\theta = 90°$ increases as the attenuation of the light doubly scattered into the backscatter directions is much smaller than that suffered by the singly scattered light collected at the same angle. Both effects are evident

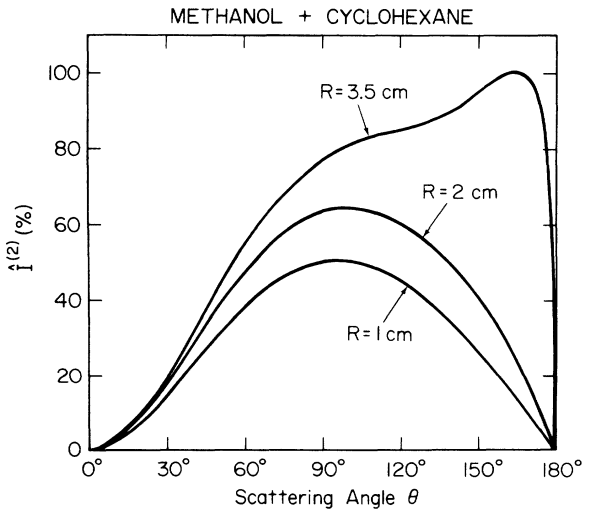

FIG. 5. Double-scattered intensity $\hat{I}^{(2)}$ for methanol + cyclohexane as a function of the scattering angle θ at various values of the radius R of the sample cell ($T - T_c = 10$ mK, $H = 0.062$ cm).

in Fig. 5. The figure reveals a second peak near $\theta = 170°$ when $R = 3.5$ cm; in this pathological case $R\tau \simeq 4$, implying that the incident beam is attenuated 99.97% as it traverses the cell. When the correlation length ξ is small and the turbidity τ is much smaller than R^{-1}, we confirm the findings of Boots *et al.*[14] and of Adzhemyan *et al.*[22] that $\hat{I}^{(2)}$ varies as $\ln(R/H)$.

In Figs. 6 and 7 we show the double-scattered intensity $\hat{I}^{(2)}$ and the depolarization ratio $\Delta^{(2)}$ for 3-methylpentane + nitroethane and methanol + cyclohexane, respectively, as a function of the temperature $\Delta T = T - T_c$ at various scattering angles. For very small $k_0\xi$, i.e., far away from T_c, the double-scattered intensity $\hat{I}^{(2)}$ varies with temperature as $t^{-\gamma}$; for large $k_0\xi$, i.e., very close to T_c, $\hat{I}^{(2)}$ varies less rapidly with temperature. From Fig. 6(b) we note that the depolarization ratio $\Delta^{(2)}$ for 3-methylpentane + nitroethane is very small at all temperatures. From Fig. 7(b) we see that the depolarization ratio $\Delta^{(2)}$ of a strong scatterer such as methanol + cyclohexane is not only large but also goes through a maximum as a function of temperature. The decrease of $\Delta^{(2)}$ at temperatures closer to T_c is due to the rapid increase of $I_{vv}^{(2)}$ [cf. (3.18)]. As mentioned earlier, at these temperatures higher-order scattering contributions will also be significant. Comparing the curves in Figs. 6 and 7 for a backscattering angle of 150° with those for a corresponding forward scattering angle of 30° illustrates enhancement of the double-scattering effects in the back-

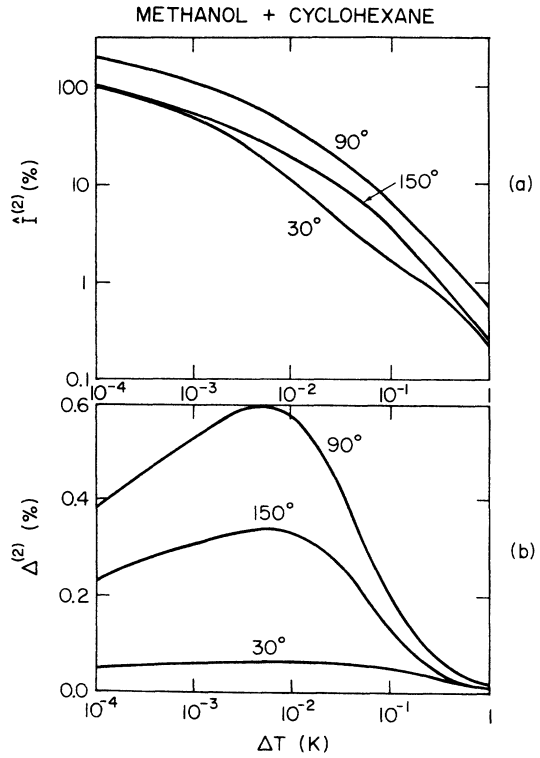

FIG. 7. Double-scattered intensity $\hat{I}^{(2)}$ and depolarization ratio $\Delta^{(2)}$ for methanol + cyclohexane as a function of $\Delta T = T - T_c$ at various values of the scattering angle θ ($R = 0.50$ cm, $H = 0.062$ cm).

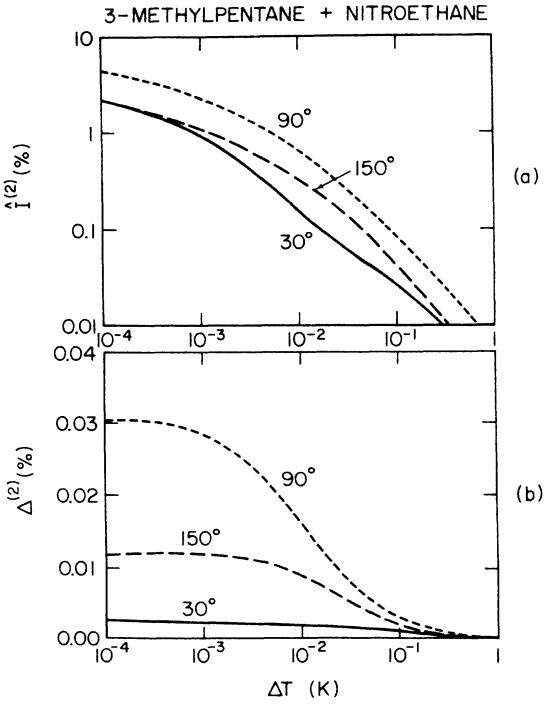

FIG. 6. Double-scattered intensity $\hat{I}^{(2)}$ and depolarization ratio $\Delta^{(2)}$ for 3-methylpentane + nitroethane as a function of $\Delta T = T - T_c$ at various values of the scattering angle θ ($R = 0.50$ cm, $H = 0.062$ cm).

scattering directions. This enhancement is particularly pronounced for the depolarization ratio $\Delta^{(2)}$.

In Figs. 8 and 9 we show the depolarization ratio $\Delta^{(2)}$ for the two liquid mixtures as a function of the aperture height H at a given temperature $\Delta T = T - T_c = 1$ mK. Previous investigators[12,13,20] have shown that the depolarization ratio $\Delta^{(2)}$ will vary linearly with the aperture height H when $\tau H \ll 1$. Our results for 3-methylpentane + nitroethane, for which τ is very small,

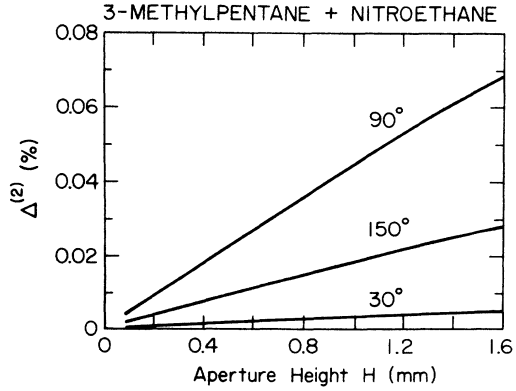

FIG. 8. The depolarization ratio $\Delta^{(2)}$ for 3-methylpentane + nitroethane as a function of the aperture height H at various scattering angles θ ($T - T_c = 1$ mK, $R = 0.50$ cm).

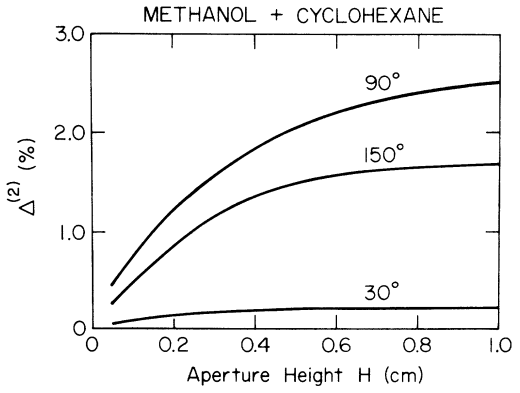

FIG. 9. The depolarization ratio $\Delta^{(2)}$ for methanol + cyclohexane as a function of the aperture height H at various scattering angles θ ($T-T_c=1$ mK, $R=0.50$ cm).

confirm this linear relation. However, when the turbidity becomes large, as is the case for methanol + cyclohexane, $\Delta^{(2)}$ has a weaker dependence on the aperture height H.

Near the critical point the inverse scattering intensity $1/I^{(1)}(\theta)$ will vary linearly with

$$k^2=4k_0^2\sin^2(\theta/2)\ .$$

Such a plot is commonly referred to as an Ornstein-Zernike (OZ) plot. In Fig. 10 we show the inverse scattering intensity as a function of k^2 for the micellar system octaethyleneglycol monododecyl ether ($C_{12}E_8$) plus water near the critical point. The dashed curve represents the experimental data obtained by Dietler and Cannell,[39] while the solid line represents the data after being corrected for double scattering. Their data are completely consistent with our calculations, which imply that double scattering reduces the apparent correlation

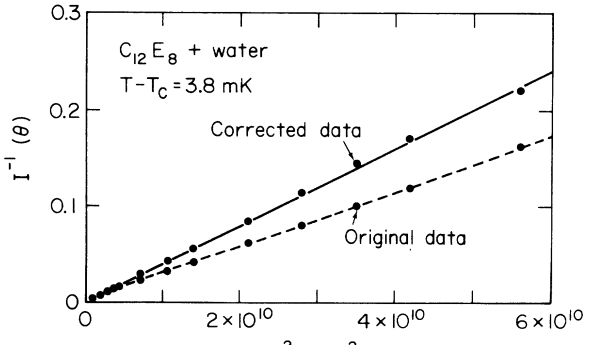

FIG. 10. Inverse scattering intensity (in arbitrary units) as a function of $k^2=4k_0^2\sin^2(\theta/2)$ for the micellar system $C_{12}E_8$ plus water near the critical point. The dashed curve represents the experimental light-scattering intensities as measured by Dietler and Cannell (Ref. 39). The solid line represents the light-scattering intensities corrrected for double-scattering contributions. The relevant physical parameters are $\xi=10\,165$ Å, $\tau=1.816$ cm^{-1}, $R=0.15$ cm, $H=0.062$ cm. The data points indicated by the arrows correspond to a scattering angle of 90°.

length (ξ_0 increases but ν decreases) and also reduces the apparent compressibility (and exponent γ). Figure 10 shows that the effects of double scattering are difficult to perceive as deviations from linearity in an OZ plot unless one makes accurate measurements at very small and very large scattering angles.

V. COMPARISON WITH EXPERIMENTS

Attempts to investigate multiple scattering experimentally have been made by Reith and Swinney[12] and by Trappeniers and co-workers[16–18] for fluids near the vapor-liquid critical point and by Adzhemyan *et al.*,[21,22] Hamano *et al.*,[19] and Schroeter *et al.*[20] for binary-liquid mixtures near the consolute point. In particular, the experiments of Hamano, Kuwahara, and Kaneko[19] appear to be suitable for a quantitative comparison with our theoretical analysis.

Hamano and co-workers measured light scattered from the binary-liquid mixture diethylmalonate + polystyrene as a function of temperature and scattering angle. Measurements were made with a small capillary cell with a radius $R=0.025$ cm and a larger cell with a radius $R=0.30$ cm. Assuming that the double-scattering contribution was negligible for the fluid in the smaller capillary cell, they then obtained experimental values of the intensity $I^{(m)}$ of multiply scattered light for the fluid in the larger cell. It turns out that the original experimental data for $I^{(m)}$ did not appear to go to zero as $\theta\to0$, as they should. In consultation with Hamano[40] this artifact was attributed to a gain calibration error leading to a correction of 3.5%. From our theory we find that the double-scattered intensity for the fluid in the smaller capillary cell is small but not negligible. Hence we corrected the experimental data for the estimated double scattering in the smaller cell; this correction was small but increased to a maximum value of 6% at the temperature closest to the critical temperature.

The experimental data for the relative intensity $\hat{I}^{(m)}=I^{(m)}/I^{(1)}$ of multiply scattered light as a function of scattering angle are shown in Fig. 11. The curves in this figure represent the double-scattered intensity $\hat{I}^{(2)}$ calculated from the equations in this paper with $R=0.30$ cm and $H=0.10$ cm. The physical parameters for diethyl malonate + polystyrene used in the calculation were earlier presented in Table I.

In order to discuss the comparison between theory and experiment the following remarks should be made. The experimental data for $I^{(m)}$ consist of the sum of the intensity $I^{(2)}$ from doubly scattered light and the intensity $I^{(h)}$ of higher-order scattered light. We expect $I^{(h)}$ to be negligible far away from T_c and to increase when T_c is approached more closely. Furthermore, we expect $I^{(h)}$ to vary less strongly with the scattering angle θ than either $I^{(1)}$ or $I^{(2)}$. Because of the anisotropy of $I^{(1)}$, the contribution $\hat{I}^{(h)}=I^{(h)}/I^{(1)}$ would increase for large scattering angles. Generally, the observed deviations between the experimental values of $\hat{I}^{(m)}$ and the theoretical values $\hat{I}^{(2)}$ are consistent with this reasoning at least for $\theta<100°$. At larger backscattering angles there are systematic deviations even at $\Delta T=T-T_c=0.8344$ K. The

anisotropy in $I^{(1)}$ and turbidity at this temperature are too small to account for this behavior and we assert (in agreement with Hamano[40]) that this phenomenon is probably due to contributions from stray light or reflected light.

We conclude that the agreement between theory and experiment is good for angles θ up to about 100°, with the exception of the data obtained at $\Delta T=0.8344$ K and 0.1240 K. Since $\lim_{\theta\to 0}\hat{I}^{(m)}(\theta)\gg 0$ at $\Delta T=0.8344$ K, we assume that the systematic mismatch at this temperature is due to a residual gain mismatch between the experiments with the smaller and larger cell. The substantial systematic deviations at $\Delta T=0.124$ K may be due in part to higher-order scattering ($2R\tau=1.5$ at this temperature), although the angular dependence of $\hat{I}^{(m)}$ for small θ suggests that a residual gain mismatch may also be present in the experiments at this temperature.

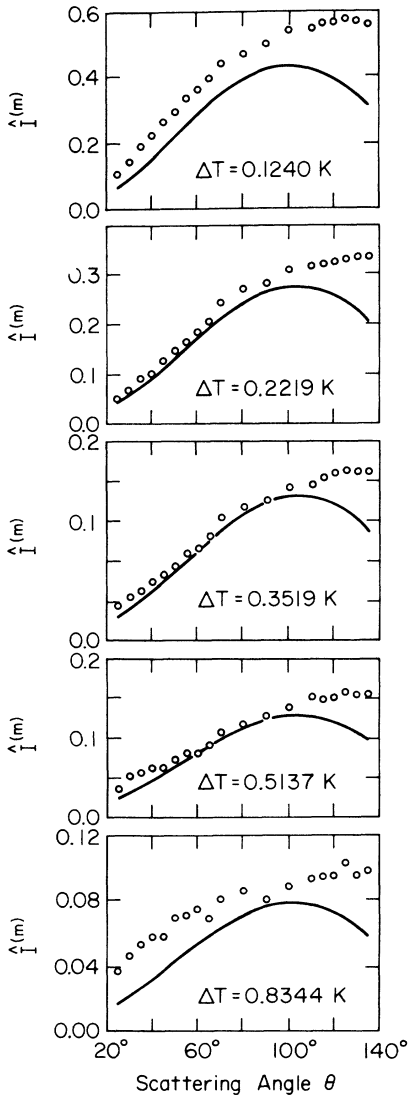

FIG. 11. Comparison between the calculated double-scattered intensity $\hat{I}^{(2)}$ (solid curves) and the experimental multiple-scattered intensities (circles) as measured by Hamano *et al.*[19] for diethylmalonate + polystyrene.

VI. DISCUSSION

In this paper we have developed a procedure for calculating the double-scattering contributions to the polarized and depolarized light-scattering intensity as a function of the scattering angle θ, taking into account the effect of the turbidity τ on the double-scattering contributions. If we restrict ourselves to $\theta=\pi/2$ and neglect the turbidity by taking $\tau=0$, our results for 3-methylpentane + nitroethane become identical to those obtained by Bray and Chang,[13] while for methanol + cyclohexane our results are consistent with the values calculated by Schroeter *et al.*[20] Furthermore, for $k_0\xi\ll 1$ and $\tau=0$ our result matches that of Boots *et al.*[41] for general angles. Thus our more complete analysis is consistent with the theoretical results obtained previously. As discussed in Sec. V our results agree within experimental accuracy with the multiple-scattering data of Hamano *et al.*,[19] as long as $2R\tau\leq 0.75$.

The following assumptions have been made in devising our basic equations for the double-scattered intensity: (a) we have neglected the finite diameter of the incident beam and the variation of the double-scattering integrand across the aperture, and (b) we have assumed that the aperture is large enough so that diffraction effects may be neglected. Here we briefly discuss these approximations.

Roughly speaking, the finite diameter of the incident beam may be neglected so long as it is much smaller than the macroscopic dimensions of the scattering cell, specifically, the radius R and the aperture height H. Bray and Chang[13] estimated the correction due to a nonzero beamwidth W_b for $\theta=90°$ and $\tau=0$ as a function of the cell dimensions and $k_0\xi$. They find that the relative correction $(\delta I^{(2)})/I^{(2)}$ to the double-scattered intensity $I^{(2)}$ for $H/2R\ll 1$ and $k_0\xi\ll 2R/H$ is given by[42]

$$(\delta I^{(2)})/I^{(2)}=\frac{f(W_b/H)}{\ln(2R/H)+D(k_0\xi)}\ , \tag{6.1}$$

where

$$f(x)=\frac{1}{2}-\frac{(1+x)^2}{4x}\ln(1+x)+\frac{(1-x)^2}{4x}\ln(1-x)\ , \tag{6.2}$$

while $D(y)$ is a function determined numerically. At $k_0\xi=2$, Eq. (6.1) yields a correction of -0.015% for the light-scattering apparatus of Haller *et al.*[5] and -0.086% for the photometer of Hamano *et al.*[19] These are small corrections indeed. The relative correction to the depolarized intensity was found by Bray and Chang to be smaller than $(4/\pi)(W_b/2R)^2$; for the light-scattering apparatus of Haller *et al.*[5] with a beamwidth $W_b=0.1$ mm this correction is less than 0.013%.

Diffraction effects have been investigated by Schroeter *et al.*[20] They conclude that the geometric-optics approximation, which has been employed in the present analysis, is valid for $A_1\simeq\sqrt{H\Delta a}\geq 0.6$ mm. This condition is satisfied for the instruments of Haller *et al.*[5] and of Hamano *et al.*[19]

In practice, the accuracy of the calculated double-scattering corrections is limited by the experimental uncertainties in the scattering strength A_0 and the dimensions H and Δa of the aperture.

ACKNOWLEDGMENTS

The authors are indebted to H. C. Burstyn, D. S. Cannell, and R. W. Gammon for many valuable discussions and to K. Hamano for providing us with details about his experimental multiple-scattering data. The research was supported by National Science Foundation Grant No. DMR-82-05356. Computer time for this project was in part supported by the Computer Science Center of the University of Maryland.

APPENDIX: EVALUATION OF THE INTEGRAND OF THE DOUBLE-SCATTERING INTEGRAL (3.10)

Our task is to compute the function $\tilde{G}(u,v,w)$, i.e., the projection of

$$G(u,v,w)=\frac{e^{\tau(u+v-\rho)}[g_{vv}(u,v,w)+g_{vh}(u,v,w)]}{(\alpha\rho-u-v\cos\theta)(\alpha\rho-v-u\cos\theta)} \tag{A1}$$

onto the even eigenstate of the parity operator in u,v,w space. We begin by decomposing the factors in $G(u,v,w)$ into parity eigenstates, for which purpose it is convenient to define

$$r^2\equiv\rho^2-w^2=u^2+v^2+2uv\cos\theta\ , \tag{A2}$$

$$s^2\equiv u^2+v^2+w^2\ , \tag{A3}$$

$$\omega=\tfrac{1}{2}\arcsin\left[\frac{2uv\cos\theta}{s^2}\right]\ , \tag{A4}$$

so that

$$\rho=s(\sin\omega+\cos\omega)\ . \tag{A5}$$

We first consider the polarization factors $g_{vv}=\rho^{-4}r^4$ and $g_{vh}=\rho^{-4}u^2w^2\sin^2\theta$ as defined by (2.16). We note that

$$\begin{aligned} r^4\,|^{(+,+)}&=(u^2+v^2)^2+4u^2v^2\cos^2\theta\ ,\\ r^4\,|^{(-,-)}&=4(u^2+v^2)uv\cos\theta\ , \end{aligned} \tag{A6}$$

$$\begin{aligned} \rho^{-4}\,|^{(+,+)}&=\frac{s^4+4u^2v^2\cos^2\theta}{(s^4-4u^2v^2\cos^2\theta)^2}\ ,\\ \rho^{-4}\,|^{(-,-)}&=\frac{-4s^2uv\cos\theta}{(s^4-4u^2v^2\cos^2\theta)^2}\ , \end{aligned} \tag{A7}$$

where the superscripts indicate the eigenvalues for reflection through the u and v axes, respectively. We only need to consider $g_{vv}^{(+,+)},g_{vv}^{(-,-)}$ and $g_{vh}^{(+,+)},g_{vh}^{(-,-)}$, for which we obtain

$$\begin{aligned} g_{vv}^{(+,+)}&=(\rho^{-4}\,|^{(+,+)})(r^4\,|^{(+,+)})+(\rho^{-4}\,|^{(-,-)})(r^4\,|^{(-,-)})\\ &=\frac{(s^4+4u^2v^2\cos^2\theta)[(u^2+v^2)^2+4u^2v^2\cos^2\theta]-16s^2(u^2+v^2)u^2v^2\cos^2\theta}{(s^4-4u^2v^2\cos^2\theta)^2}\ , \end{aligned} \tag{A8a}$$

$$g_{vv}^{(-,-)}=\frac{4uvw^2\cos\theta[(u^2+v^2)^2+w^2(u^2+v^2)-4u^2v^2\cos^2\theta]}{(s^4-4u^2v^2\cos^2\theta)^2}\ , \tag{A8b}$$

$$g_{vh}^{(+,+)}=\frac{u^2w^2\sin^2\theta(s^4+4u^2v^2\cos^2\theta)}{(s^4-4u^2v^2\cos^2\theta)^2}\ , \tag{A9a}$$

$$g_{vh}^{(-,-)}=\frac{-4s^2u^3vw^2\cos\theta\sin^2\theta}{(s^4-4u^2v^2\cos^2\theta)^2}\ . \tag{A9b}$$

The decomposition of the remaining factors in (2.15) proceeds in a like manner, although the presence of even-odd and odd-even terms make the manipulations more tedious. Defining

$$\Omega\equiv\sin\omega-\cos\omega\ , \tag{A10}$$

the exponential term in (2.15) may be expressed as

$$e^{\tau(u+v-\rho)}=E_{+,+}+E_{-,-}+E_{+,-}+E_{-,+}\ , \tag{A11}$$

$$\begin{aligned} E_{+,+}&=\tfrac{1}{2}\{e^{-\tau\rho}\cosh[\tau(u+v)]+e^{\tau s\Omega}\cosh[\tau(u-v)]\}\ ,\\ E_{-,-}&=\tfrac{1}{2}\{e^{-\tau\rho}\cosh[\tau(u+v)]-e^{\tau s\Omega}\cosh[\tau(u-v)]\}\ ,\\ E_{+,-}&=\tfrac{1}{2}\{e^{-\tau\rho}\sinh[\tau(u+v)]-e^{\tau s\Omega}\sinh[\tau(u-v)]\}\ ,\\ E_{-,+}&=\tfrac{1}{2}\{e^{-\tau\rho}\sinh[\tau(u+v)]+e^{\tau s\Omega}\sinh[\tau(u-v)]\}\ . \end{aligned} \tag{A12}$$

The Ornstein-Zernike factor in (2.15) separates as

$$\frac{1}{(\alpha\rho-u-v\cos\theta)(\alpha\rho-v-u\cos\theta)}=D_{+,+}+D_{-,-}+D_{+,-}+D_{-,+}\ , \tag{A13}$$

where the terms $D_{\pm,\pm}$ are defined by the following set of equations:

$$\begin{aligned} B_{+,+}&=\alpha^2s^2+(u^2+v^2)\cos\theta\ ,\\ B_{-,-}&=uv(1+2\alpha^2\cos\theta+\cos^2\theta)\ ,\\ B_{+,-}&=-\alpha s(u\sin\omega+v\cos\omega)(1+\cos\theta)\ ,\\ B_{-,+}&=-\alpha s(u\cos\omega+v\sin\omega)(1+\cos\theta)\ , \end{aligned} \tag{A14}$$

$$\begin{aligned} C_{+,+}&=B_{+,+}^2-B_{-,-}^2+B_{+,-}^2-B_{-,+}^2\ ,\\ C_{+,-}&=2(B_{+,+}B_{+,-}-B_{-,-}B_{-,+})\ , \end{aligned} \tag{A15}$$

$$D_{+,+}=\frac{B_{+,+}C_{+,+}-B_{+,-}C_{+,-}}{C_{+,+}^2-C_{+,-}^2}\ ,\qquad D_{+,-}=\frac{B_{+,-}C_{+,+}-B_{+,+}C_{+,-}}{C_{+,+}^2-C_{+,-}^2}\ ,$$

$$D_{-,-}=\frac{B_{-,+}C_{+,-}-B_{-,-}C_{+,+}}{C_{+,+}^2-C_{+,-}^2}\ ,\qquad D_{-,+}=\frac{B_{-,-}C_{+,-}-B_{-,+}C_{+,+}}{C_{+,+}^2-C_{+,-}^2}\ . \tag{A16}$$

For $\tilde{G}(u,v,w)=G^{(+,+)}(u,v,w)$ we then obtain

$$\begin{aligned}\tilde{G}(u,v,w)=&\tfrac{1}{4}e^{\pi(u+v-\rho)}(g_{+,+}+g_{-,-})(D_{+,+}+D_{-,-}+D_{+,-}+D_{-,+})\\&+\tfrac{1}{4}e^{-\pi(u+v+\rho)}(g_{+,+}+g_{-,-})(D_{+,+}+D_{-,-}-D_{+,-}-D_{-,+})\\&+\tfrac{1}{4}e^{\pi(u+v-\rho\Delta)}(g_{+,+}-g_{-,-})(D_{+,+}-D_{-,-}-D_{+,-}+D_{-,+})\\&+\tfrac{1}{4}e^{-\pi(u-v+\rho\Delta)}(g_{+,+}-g_{-,-})(D_{+,+}-D_{-,-}+D_{+,-}-D_{-,+})\end{aligned} \tag{A17}$$

with

$$\Delta\equiv\left[1-\frac{4uv\cos\theta}{\rho^2}\right]^{1/2}\ . \tag{A18}$$

The functions $g_{+,+},g_{-,-}$ in (A17) should be identified with $g_{vv}+g_{vh}$ for calculating the total double-scattering intensity and with g_{vv} and g_{vh} separately for calculating the polarized and depolarized components. The function $\tilde{G}(u,v,w)$ carries the unit of l^{-2} and is proportional to ρ^{-2} in the new coordinates.

Finally, the integrand

$$\tilde{F}(\rho,\delta,\psi)=\rho^2\sin\delta\,\tilde{G}(u(\rho,\delta,\psi),v(\rho,\delta,\psi),w(\rho,\delta)) \tag{A19}$$

of the double-scattering integral is written in the form

$$\tilde{F}(\rho,\delta,\psi)=\sum_{i=1}^{4}e^{\rho\tau H_i(\delta,\psi)}[J_{vv}^{(i)}(\delta,\psi)+J_{vh}^{(i)}(\delta,\psi)]\ , \tag{A20}$$

where the functions $H_i(\delta,\psi)$, $J_{vv}^{(i)}\delta,\psi)$, and $J_{vh}^{(i)}(\delta,\psi)$ are defined by

$$\begin{aligned}H_1(\delta,\psi)&=\frac{\sin\delta}{\sin\theta}[\cos(\psi+\psi_0)+\sin(\psi-\psi_0)]-1\ ,\\H_2(\delta,\psi)&=\frac{\sin\delta}{\sin\theta}[-\cos(\psi+\psi_0)-\sin(\psi-\psi_0)]-1\ ,\\H_3(\delta,\psi)&=\frac{\sin\delta}{\sin\theta}[\cos(\psi+\psi_0)-\sin(\psi-\psi_0]-\Delta\ ,\\H_4(\delta,\psi)&=\frac{\sin\delta}{\sin\theta}[-\cos(\psi+\psi_0)+\sin(\psi-\psi_0)]-\Delta\ ,\end{aligned} \tag{A21}$$

$$\begin{aligned}J_{vv}^{(1)}(\delta,\psi)=&\tfrac{1}{4}\sin\delta(g_{vv}^{(+,+)}+g_{vv}^{(-,-)})\\&\times(D_{+,+}+D_{-,-}+D_{+,-}+D_{-,+})\rho^2\ ,\\J_{vh}^{(1)}(\delta,\psi)=&\tfrac{1}{4}\sin\delta(g_{vh}^{(+,+)}+g_{vh}^{(-,-)})\\&\times(D_{+,+}+D_{-,-}+D_{+,-}+D_{-,+})\rho^2\ ,\end{aligned} \tag{A22}$$

$$\begin{aligned}J_{vv}^{(2)}(\delta,\psi)=&\tfrac{1}{4}\sin\delta(g_{vv}^{(+,+)}+g_{vv}^{(-,-)})\\&\times(D_{+,+}+D_{-,-}-D_{+,-}-D_{-,+})\rho^2\ ,\\J_{vh}^{(2)}(\delta,\psi)=&\tfrac{1}{4}\sin\delta(g_{vh}^{(+,+)}+g_{vh}^{(-,-)})\\&\times(D_{+,+}+D_{-,-}-D_{+,-}-D_{-,+})\rho^2\ ,\\J_{vv}^{(3)}(\delta,\psi)=&\tfrac{1}{4}\sin\delta(g_{vv}^{(+,+)}-g_{vv}^{(-,-)})\\&\times(D_{+,+}-D_{-,-}-D_{+,-}+D_{-,+})\rho^2\ ,\\J_{vh}^{(3)}(\delta,\psi)=&\tfrac{1}{4}\sin\delta(g_{vh}^{(+,+)}-g_{vh}^{(-,-)})\\&\times(D_{+,+}-D_{-,-}-D_{+,-}+D_{-,+})\rho^2\ ,\end{aligned} \tag{A23}$$

$$\begin{aligned}J_{vv}^{(4)}(\delta,\psi)=&\tfrac{1}{4}\sin\delta(g_{vv}^{(+,+)}-g_{vv}^{(-,-)})\\&\times(D_{+,+}-D_{-,-}+D_{+,-}-D_{-,+})\rho^2\ ,\\J_{vh}^{(4)}(\delta,\psi)=&\tfrac{1}{4}\sin\delta(g_{vh}^{(+,+)}-g_{vh}^{(-,-)})\\&\times(D_{+,+}-D_{-,-}+D_{+,-}-D_{-,+})\rho^2\ .\end{aligned}$$

Since as mentioned earlier, the functions $D_{\pm,\pm}$ are inversely proportional to ρ^2, we evaluate the integrand in practice by taking

$$\begin{aligned}&D_{\pm,\pm}(u(\rho,\delta,\psi),v(\rho,\delta,\psi),w(\rho,\delta))\rho^2\\&\quad=D_{\pm,\pm}(u(1,\delta,\psi),v(1,\delta,\psi),w(1,\delta))\ .\end{aligned} \tag{A24}$$

*Present address: Department of Physics, University of California at Santa Barbara, Santa Barbara, CA 93106.

[1]B. Chu, Annu. Rev. Phys. Chem. **21**, 145 (1974).

[2]W. I. Goldburg, in *Light Scattering near Phase Transitions*, edited by H. Z. Cummins and A. P. Levanyuk (North-Holland, Amsterdam, 1983), p. 531.

[3]D. McIntyre and J. V. Sengers, in *Physics of Simple Liquids*, edited by H. N. V. Temperley, J. S. Rowlinson, and G. S. Rushbrooke (North-Holland, Amsterdam, 1968), p. 447.

[4]K. Hamano, N. Kuwahara, M. Nakata, and M. Kaneko, Phys. Lett. **63A**, 121 (1977).

[5]H. Haller, C. Destor, and D. S. Cannell, Rev. Sci. Instrum. **54**, 973 (1983).

[6]R. F. Chang, H. Burstyn, and J. V. Sengers, Phys. Rev. A **19**, 866 (1979).

[7]H. C. Burstyn and J. V. Sengers, Phys. Rev. A **25**, 448 (1982).

[8]H. C. Burstyn and J. V. Sengers, Phys. Rev. A **27**, 1085 (1983).
[9]R. B. Kopelman, R. W. Gammon, and M. R. Moldover, Phys. Rev. A **29**, 2048 (1984).
[10]D. W. Oxtoby and W. M. Gelbart, J. Chem. Phys. **60**, 3359 (1974).
[11]D. W. Oxtoby and W. M. Gelbart, Phys. Rev. A **10**, 738 (1974).
[12]L. A. Reith and H. L. Swinney, Phys. Rev. A **12**, 1094 (1975).
[13]A. J. Bray and R. F. Chang, Phys. Rev. A **12**, 2594 (1975).
[14]H. M. J. Boots, D. Bedeaux, and P. Mazur, Physica **84A**, 217 (1976).
[15]H. M. J. Boots, Physica **87A**, 185 (1977).
[16]N. J. Trappeniers, A. C. Michels, H. M. J. Boots, and R. H. Huyser, Physica **101A**, 431 (1980).
[17]N. J. Trappeniers, H. M. J. Boots, R. W. Huyser, and A. C. Michels, Physica **103A**, 455 (1980).
[18]N. J. Trappeniers, R. H. Huyser, A. C. Michels, and H. M. J. Boots, Physica **126A**, 116 (1984).
[19]K. Hamano, N. Kuwahara, and M. Kaneko, Phys. Rev. A **21**, 1312 (1980).
[20]J. P. Schroeter, D. M. Kim, and R. Kobayashi, Phys. Rev. A **27**, 1134 (1983).
[21]L. V. Adzhemyan, L. Ts. Adzhemyan, L. A. Zubkov, and V. P. Romanov, Zh. Eksp. Teor. Fiz. **78**, 1051 (1980) [Sov. Phys.—JETP **51**, 530 (1980)].
[22]L. V. Adzhemyan, L. Ts. Adzhemyan, L. A. Zubkov, and V. P. Romanov, Zh. Eksp. Teor. Fiz. **80**, 551 (1981) [Sov. Phys.—JETP **53**, 278 (1981)].
[23]E. L. Lakoza and A. V. Chalyi, Zh. Eksp. Teor. Fiz. **82**, 441 (1982) [Sov. Phys.—JETP **55**, 252 (1982)].
[24]M. R. Moldover, J. V. Sengers, R. W. Gammon, and R. J. Hocken, Rev. Mod. Phys. **51**, 79 (1979).
[25]C. M. Sorensen, R. C. Mockler, and W. J. O'Sullivan, Opt. Commun. **20**, 140 (1977).
[26]C. M. Sorensen, R. C. Mockler, and W. J. O'Sullivan, Phys. Rev. A **16**, 365 (1977).
[27]D. Beysens and G. Zalczer, Phys. Rev. A **15**, 765 (1977).
[28]R. A. Ferrell and J. K. Bhattacharjee, Phys. Rev. A **19**, 348 (1979).
[29]V. P. Romanov and T. K. Salikhov, Opt. Spektrosk. **58**, 1091 (1985) [Opt. Spectrosc. (USSR) **58**, 666 (1985)].
[30]L. D. Landau and E. M. Lifshitz, *Electrodynamics of Continuous Media* (Addison-Wesley, Reading, MA, 1960).
[31]B. J. Berne and R. Pecora, *Dynamic Light Scattering* (Wiley, New York, 1976).
[32]M. E. Fisher, J. Math. Phys. **5**, 944 (1964).
[33]V. G. Puglielli and N. C. Ford, Phys. Rev. Lett. **25**, 143 (1970).
[34]J. G. Shanks, Ph.D. thesis, University of Maryland, 1986.
[35]P. Wiltzius and D. S. Cannell (private communication).
[36]J. V. Sengers and J. M. H. Levelt Sengers, Annu. Rev. Phys. Chem. **37**, 189 (1986).
[37]B. Chu, J. Phys. Chem. **67**, 1969 (1963).
[38]D. T. Jacobs, Phys. Rev. A **33**, 2605 (1986).
[39]G. Dietler and D. S. Cannell, Phys. Rev. Lett. **60**, 1852 (1988).
[40]K. Hamano (private communication).
[41]Reference 14, Eq. (6.5).
[42]Reference 13, Eq. (A8).